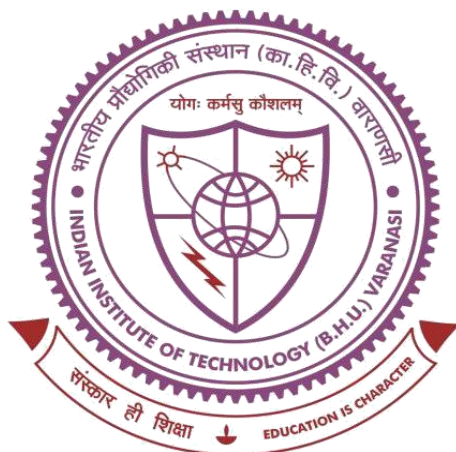


**DEVELOPMENT AND CHARACTERIZATION OF NOVEL
PHYTOFORMULATIONS FOR MELANOMA THERAPY**



**Thesis submitted in partial fulfillment for the
Award of Degree**

Doctor of Philosophy

By

Debadatta Mohapatra

**DEPARTMENT OF PHARMACEUTICAL ENGINEERING & TECHNOLOGY
INDIAN INSTITUTE OF TECHNOLOGY
(BANARAS HINDU UNIVERSITY)
VARANASI – 221005
INDIA**


Roll No- 19161016

Year 2023

CERTIFICATE

It is certified that the work contained in the thesis titled ***“Development and characterization of novel phytoformulations for melanoma therapy”*** by **Mr. Debadatta Mohapatra** has been carried out under my supervision and that this work has not been submitted elsewhere for a degree.

It is further certified that the student has fulfilled all the requirements of Comprehensive Examination, Candidacy and SOTA for the award of Ph.D. degree.



Dr. Alakh N Sahu
Supervisor

अलेख एन साहु / Alakh N. Sahu
सह आचार्य / Associate Professor
भैषजकीय अभियांत्रिकी एवं तैद्योगिकी विभाग/
Department of Pharmaceutical Engineering & Technology
भारतीय प्रौद्योगिकी संस्थान Indian Institute of Technology
(काशी हिन्दू विश्वविद्यालय)/(Banaras Hindu University)
वाराणसी-२२१००५/Varanasi-221005
E-mail:ansahu.phe@iitbhu.ac.in

DECLARATION BY THE CANDIDATE

I, "**Debadatta Mohapatra**", certify that the work embodied in this thesis is my own bonafide work and carried out by me under the supervision of "**Dr. Alakh N Sahu**" from "**July 2019**" to "**October 2023**", at the "**Department of Pharmaceutical Engineering & Technology**", Indian Institute of Technology (BHU), Varanasi. The matter embodied in this thesis has not been submitted for the award of any other degree/diploma. I declare that I have faithfully acknowledged and given credits to the research workers wherever their works have been cited in my work in this thesis. I further declare that I have not willfully copied any other's work, paragraphs, text, data, results, etc., reported in journals, books, magazines, reports dissertations, theses, etc., or available at websites and have not included them in this thesis and have not cited as my own work.

Date: 20.10.2023

Place: Varanasi

Debadatta Mohapatra
Debadatta Mohapatra

CERTIFICATE BY THE SUPERVISOR

It is certified that the above statement made by the student is correct to the best of my knowledge.

Dr. Alakh N Sahu
20.10.2023
Dr. Alakh N Sahu
Supervisor

अलेख एन साहु / Alakh N. Sahu
सह आचार्य / Associate Professor
भैषजकीय अभियांत्रिकी एवं प्रौद्योगिकी विभाग/
Department of Pharmaceutical Engineering & Technology
भारतीय प्रौद्योगिकी संस्थान-Indian Institute of Technology
(काशी हिन्दू विश्वविद्यालय)/(Banaras Hindu University)
वाराणसी-२२१००५/Varanasi-221005
E-mail:ansahu.phe@iitbhu.ac.in

S. Hemalatha
Prof. S. Hemalatha
Head of the Department
विभागाध्यक्ष / Head

भैषजकीय अभियांत्रिकी एवं प्रौद्योगिकी विभाग /
Department of Pharmaceutical Engineering & Technology
भारतीय प्रौद्योगिकी संस्थान / INDIAN INSTITUTE OF TECHNOLOGY
(बनारस हिन्दू विश्वविद्यालय) / (BANARAS HINDU UNIVERSITY)
वाराणसी-२२१००५ / Varanasi-221005

COPYRIGHT TRANSFER CERTIFICATE

Title of the Thesis: Development and characterization of novel phytoformulations for melanoma therapy

Name of the Student: Debadatta Mohapatra

COPYRIGHT TRANSFER

The undersigned hereby assigns to the Indian Institute of Technology (Banaras Hindu University), Varanasi, all rights under copyright that may exist in and for the above thesis submitted for the award of the "*Doctor of Philosophy*".

Date: 20.10.2023

Place: Varanasi


Debadatta Mohapatra

Note: However, the author may reproduce or authorize others to reproduce material extracted verbatim from the thesis or derivative of the thesis for author's personal use provided that the source and the Institute's copyright notice are indicated.

ACKNOWLEDGEMENT

*With humility, misty eyes, and folded hands, I sincerely acknowledge my gratitude to the Almighty for showering his blessings upon me. I would like to thank the God of wisdom, knowledge, and prosperity “**Lord Ganesha Ji,**” Deva Deva Mahadeva “**Kashi Vishwanath Ji,**” Lord of the Universe “**Lord Jagannath Ji**” for showering their continuous blessings. The Almighty constantly infused me with the strength and concentration to embark on and accomplish this work successfully. This research work would not be possible without their benediction and grace. I pray that this hidden force always blesses me with the strength, courage, wisdom, and willpower to face all the challenges of life.*

I am grateful to all those guides of righteous path from whom the sources of actuality are alive even today. Gratitude is the fundamental value for progression towards awakening. Gratitude itself is the foundation and conserving value for culture and civilization.

One who is not grateful cannot produce evidence of bearing culture and civilization. One who does not bear culture and civilization cannot follow norms and orderliness.

Culture, Civilization, Norms, and Orderliness are mutually complementary. Without these, it is not possible to determine the Undivided society and Social harmony. Therefore –without gratitude, honour is not; without honour simplicity is not; without simplicity, coexistence is not; without coexistence, continuity of gratitude is not.

The human being who lives with gratitude, only his conduct is educative and inspiring for future generations. This is achievable only in the purview of Humanness. Gratitude is for all those who have been helpful, in whichever way, towards Consciousness Development – Value Education.

*My first and foremost heartfelt gratitude and indebtedness would be towards “**Bharat Ratna Mahamana Pandit Madan Mohan Malviya Ji,**” the founder of Banaras Hindu University, for establishing a magnificent temple of learning. I am extremely grateful to “**Prof. Mahadeva Lal Schroff,**” the father of Indian pharmacy education, for his great contributions to the field of pharmacy towards the introduction of Bachelor's and Master Degree courses in the Discipline of Pharmaceutical Sciences in India.*

*I would like to express a deep sense of gratitude, appreciation, and indebtedness to my honourable supervisor **Dr. Alakh N. Sahu**, for providing his continuous support, motivation, and immense knowledge towards the conceptualization, experiment designing, project investigation, supervision, data interpretation, expert assistance, editing, drafting, and revision functions. His professional acumen, plausible and erudite thinking, and perfect counseling helped me in achieving my goal. His meticulous ways, utmost attention to all problems, continuous involvement, precious guidance, valued suggestions, and tireless efforts made this immense task come to a conclusion successfully. I am also thankful to him for providing the necessary facilities to carry out this research work. I feel fortunate to have been associated with and worked under such an accomplished personality.*

*I would also like to thank my Research Progress Evaluation Committee (RPEC) members, **Prof. Abha Mishra** (Professor, School of Biochemical Engineering, IIT (BHU), Varanasi) and **Dr. Ashish Kumar Agrawal** (Associate Professor, Department of Pharmaceutical Engineering and Technology, IIT (BHU), Varanasi) for their valuable guidance, supervision, expert assistance, scientific inputs, and suggestions throughout the experiments.*

*I express my gratitude to **Prof. Siva Hemalatha**, Head, Department of Pharmaceutical Engineering & Technology, I.I.T. (B.H.U.), Varanasi, for providing the necessary facilities and academic guidance during my Ph.D. work. I am immensely thankful to all former Head of the Department, **Prof. Brahmeshwar Mishra**, **Prof. Sushil Kumar Singh**, **Prof. Sanjay Singh**, and **Prof. Sushant Kumar Shrivastava**, for their cooperation during my research work.*

*I express my gratitude to all the faculty members and scientific officer of the Department of Pharmaceutical Engineering & Technology: **Prof. Sairam Krishnamurthy**, **Prof. Senthil Raja A.**, **Dr. Ruchi Chawla**, **Prof. M. S. Muthu**, **Dr. Sunil K Mishra**, **Dr. Prasanta K. Nayak**, **Dr. Gyan Prakash Modi**, **Dr. Vinod Tiwari**, **Dr. Ashish K Agrawal**, **Dr. Rajnish**, **Dr. Deepak Kumar**, **Dr. Dinesh Kumar**, **Dr. Jairam Meena**, **Dr. Ashok Kumar**, and **Dr. Arun Khatri** for their co-operation, and scientific suggestions during my research work. My access to their Laboratory for various works during my Ph.D. works is highly acknowledged. Without their precious support, it would not have been possible to execute this research work.*

*The efforts of the non-teaching office staff **Mr. Yashwant Singh, Mr. Atul Kumar Gupta, Mr. Anand Kumar, Mr. Bipin Kumar Pandey, Mr. Surya Pratap Singh, Mr. Kapil Dev Rai, Smt. Archana Singh, Mr. Madan Lal, Mr. Virendra Kumar, Mr. Arun Kumar, Mr. Mohd. Jameel, Mr. Akhila Nand Upadhyay, Mr. Lakshminarayan Dhara, Mr. Sunil Kumar Singh, Mr. Amit Kumar, Mr. Ram Jiyawan, Km. Shyamali Ghosal, Mr. Nand Lal, Mr. Chhote Lal, Mr. Ram Hriday Pathak, and Mr. Rafique Ahmad** of the Department could never go unnoticed, who continuously lent their support and technical assistance during the tenure of the research.*

*I wish to express deep gratitude to **Dr. Avanish Singh Parmar** (Associate Professor, Department of Physics, IIT (BHU), Varanasi), **Dr. Pawan K. Dubey** (Associate Professor, Centre for Genetics Disorders, Institute of Science (BHU), Varanasi), **Mr. Dhananjay Panigrahi** (Tech Lead, Dr. Reddy's Laboratories, Hyderabad, Telangana, India), **Dr. Pratap Chandra Acharya** (Assistant Professor, Department of Pharmacy, Tripura University (A Central University), Tripura), **Prof. Gopal Nath** (Department of Microbiology, IMS (BHU), Varanasi), **Prof. G. B. Jena** (Professor, Department of Pharmacology & Toxicology, NIPER, Mohali), **Dr. Narender Tadigoppula** (Chief Scientist, Division of Medicinal and Process Chemistry, CDRI, Lucknow), **Dr. Shantibhusan Senapati** (Scientist-E, Institute of Life Sciences, Bhubaneswar), **Dr. Sunday O. Otimenyin** (Department of Pharmacology, Faculty of Pharmaceutical Sciences, University of Jos, Jos, Plateau State, Nigeria), and **Prof. Subrat Kumar Bhattamisra** (Professor, GITAM (Deemed to be University), Andhra Pradesh, India) for providing the technical inputs during the research work.*

*I am thankful to **Mr. Dulla Naveen Kumar, Dr. Ravi Pratap, Dr. Md. Bayazeed Alam, and Dr. Vivek Pandey** for their collaborative work. My heartiest thanks to my lab mates at the Phytomedicine Research laboratory: **Mr. Dharmendra Yadav, Dr. Shreya H. Singh, Dr. Gaurav Gopal Naik, Mr. Sagar, Ms. Himani, Ms. Reena Madhavi, Mr. Pradeep Patel, Ms. Pooja Kathait, Ms. Soki Daeme Malang, Ms. Shambhavi, and Mr. Ankur** for making wonderful friendly environment in lab which made my work fruitful and enjoyable. They always had a friendly attitude and, at the same time, provided me with valuable suggestions, which helped me in carrying out my research work.*

My thankful regards to my batch mates Ms. Poorvi Saraf, Mr. K Venkateswarlu, Mr. Abhishesh Kumar Mehata, Mr. Akash Verma, Mr. Manish Kumar, Mr. Ravi Singh, Mr. Abhishek Jha, Mr. Gajendra T A, Ms. Neha Singh, Mr. Narendra, Ms. Nivedita Bhardwaj, Ms. Nancy Tripathi, Ms. Bhagwati Bhardwaj, Mr. Rangan Mitra, Ms. Gadepalli Anagha, Ms. Mohini Mishra, Mr. Swapan Maity, Ms. Divya Pareek, Ms. Sukanya Patra, and Ms. Shubhangi for their pleasant company, cooperation, and help during research work.

I am also thankful to my respected seniors, friends, and beloved juniors of the Department: Mr. Amit Singh, Mr. Tarkeshwar Dubey, Mrs. Sangita Hazarika, Dr. Kancharla Bhanukiran, Mrs. Vineeta Tiwari, Mrs. Deepa Dehari, Dr. Rinki Varma, Dr. Datta Pawde, Mr. Dharmanath Parbat, Mr. Himanshu Verma, Mr. Bhanuranjan Das, Mr. Anurag Tk Baidya, Mr. Alen T Mathew, Ms. Aiswarya Chaudhuri, Mr. Rohan Sahu, Ms. Abhipsa Mohapatra, Mr. Sanchit Arora, Ms. Udit Shiromani, Ms. Komal Rani, Ms. Sourav Bera, Ms. Vaishali Saini, Mr. Sunil Kumar, Mr. Himanshu Rai, Mr. Gaurav Singh, Mr. Kshirod Kumar Das, Ms. Km Deeksha Nigam, Ms. Aditi Tripathi, Ms. Karnika Tiwari, Mr. Govind Kumar Kachhava, Ms. Mayuri Purushottam Sawarkar, Mr. Gajanan Arjunrao Pawar, Mr. Jatin, Ms. Andarghiske Komal Rajesh, Mr. Manjeet Kumar Sah Gond, Ms. Rinki Jiwnani, Mr. Chinmaya Kumar Khuntia, Mr. Amit Maity, Mr. Chhatra Ram, Mr. Rohit Patil, Ms. Bharti Devi, Mr. Abhishek R. Mali, Mr. Souvik Mistri, and Mr. Gauransh Mishra for their healthy company, cooperation and devoting their valuable time in tailoring my work whenever required.

My heartiest thanks to Mrs. Saibani Sahu, Late. Mr. Gadadhar Sahu, Mrs. Manasi Sahu, Ms. Aditi Sahu, and Ms. Anandi Sahu for providing care, affection, and moral support as family members.

I express my gratitude to all of my respected B. Pharm and M. Pharm Teachers, especially Prof. Prakash Chandra Senapati and Prof. Gyanada Sankar Dash, Sri Jayadev College of Pharmaceutical Sciences, Bhubaneswar, Odisha, for their support and encouragement in studying for Ph.D. in this renowned Department of Pharmaceutical Engineering & Technology, IIT (BHU), Varanasi.

My special thanks to my B. Pharm and M. Pharm Batchmates, especially Mr. Bijan Kumar Mohanty, Mr. Subhra Sailendra Mishra, Mr. Subir Kumar Patra, Mr. Satya Narayan Dash, Mr. Sarada Prasad Tripathy, Mr. Prasant Sagar, Mr. MD Sonu, Ms. Itishree Aradhana Mohanty, Mr. Suchindra Bishwal, Mr. Nigam Panda, Mr. Tushar Das, Mr. Sanat Kumar Mishra, and Mr. Jyotiranjana Parida for their care, love, and mental support during my Ph.D. journey.

My heartiest thanks to all my respected seniors, especially Mr. Satyabrata Sahoo, Mr. Priyabrata Panigrahi, Mr. Satyajeet Bishwal, Mr. Smruti Ranjan panda, Mr. Bishwajeeban Barik, Mrs. Aliva Minz, and juniors Mr. Abinash Samantray, Mr. Debasis Sahoo, Mr. Swadhin Kumar Lenka, Mr. Krushna Chandra Maharana, Mr. Sanat Kumar Dash, Mr. Pravas Ranjan Dash, Mr. Kalpataru Behera, Mr. Binaya Ranjan Dash, and Mr. Kuna Das.

I am thankful to all of my 12th friends especially Mr. Chitaranjan Roul, Mr. Sambit Choudhury, Mr. Sunil Samantaray, Ms. Sushree Nibedita Rout, Ms. Ankita Biswal, Ms. Madhusmita Sahoo, and Ms. Bhagyashree Pradhan, my 10th school friends especially Mr. Bishwaranjan Swain, Mr. Pravanjan Swain, Mr. Budhadev Rout, Mr. Tapan Das, Mr. Deepak Das, Mr. Akash Samal, Ms. Sunita Swain, and Ms. Ankita Pradhan for providing support, care and mental strength during the journey.

I am very much thankful to all the members of Odia Society of Varanasi (Varanaseya Utkal Samaj) especially Prof. Gopabandhu Mishra, Prof. Kalyan Ghadei, Dr. Amiya Kumar Samal, Mrs. Sonali Mohapatra, Dr. Soumya Ranjan Meher, Dr. Siva Prasad B N V, Mr. Saroj Kanta Behera, Mr. Biswajit Mishra, Mr. Anirbana Parida, Mr. Chinmaya Chiranjeeb Nayak, Ms. Sarita Lenka, Ms. Niharika Samantaray, Ms. Bhubaneswari Sahoo, Ms. Jyotirmayee, Ms. Madhumita Priyadarsini, Ms. Saswati Dehury, Mr. Vineet Bharadwaj, Ms. Anwesha Patnaik, Ms. Ankita Nayak, Ms. Sonali Priyadarsini Sahoo, Ms. Baishnabi Kishan, Ms. Niharika Mishra, Ms. Swetasoma Nayak, Mr. Soumya Ranjan Sahoo, Mr. Ritik Roshan Parida, Mr. Pratik Biswal, Mr. Tikun Dhal, Mr. Abhijit Sahoo, Mr. Bikash Behera, Mr. Balaram Sahoo, Mr. Abhinandan Sahoo, Ms. Aishwarya Rath, Ms. Anuska Beura, Ms. Suprava Mishra, Mrs. Jhuna Rani Ojha, and Ms. Twinkle Pradhan for their care, affection, and moral support like my family members.

Finally, I shall always remain thankful and indebted to my parents, **Mr. Gouttam Mohapatra** and **Mrs. Jayalaxmi Mohapatra** and my brother **Mr. Shubhadatta Mohapatra**, and family members **Late Mr. Gopinath Mohapatra**, **Mrs. Diptimayi Pradhan**, **Mr. Kedar Swain**, **Mr. Chandrabhanu Gahan**, **Mrs. Padmini Gahan**, **Mr. Debaraj Pradhan**, **Ms. Pragyan Paramita Swain**, and **Ms. Pravati Swain**, my relatives **Ms. UB Bishnupriya**, **Mr. Asutosh Sahoo**, **Ms. Rosalin Swain**, **Mr. Omprakash Swain**, **Mrs. Meera Dubey**, and **Mrs. Shweta Dubey** for all their selflessly sacrifices, love, support, strength, and cooperation during the study. This work could not have been completed without their blessings. I have no words to thank them all.

Last but not least, I am grateful and would like to **thank everybody** who some or the other who contributed to this research work and motivated me to overcome hurdles during this journey.

The financial assistance for this work provided as a scholarship to me by the **Ministry of Human Resource Development (MHRD)**, Government of India, is highly acknowledged. I greatly acknowledge the **Central Instrumentation Facility at IIT (BHU), Varanasi**, for providing the facility for various analysis.

I am very much thankful to the **instrumental and infrastructure facilities** provided by the **Department of Pharmaceutical Engineering & Technology, IIT (BHU), Varanasi**; **Central Instrument Facility, IIT (BHU), Varanasi**; **Department of Physics, IIT (BHU), Varanasi**; and **Centre for Genetics Disorders, Institute of Science, Banaras Hindu University, Varanasi, India**.

Lastly, I pray to Almighty for the '**Moksha**' of all the **experimental animals** utilized in my experiments during the tenure of my research work.

Ultimately, I would like to bow down and pray to the **Almighty** for always giving me enough strength and courage to fulfill all my dreams and goals.

Date: 20.10.2023

Place: Varanasi


Debadatta Mohapatra

Table of contents

List of Figures.....	XVI
List of Tables.....	XXIV
List of Abbreviations.....	XXVI
List of symbols.....	XXXVI
Preface.....	XXXVIII
1 CHAPTER 1: INTRODUCTION.....	1
2 CHAPTER 2: LITERATURE REVIEW.....	9
2.1 Skin cancer and melanoma	9
2.1.1 Risk Factors	13
2.1.2 Diagnosis.....	13
2.1.3 Progression of melanoma.....	14
2.1.4 Types of melanomas	15
2.1.5 Pathogenesis.....	15
2.1.6 Current treatment strategies for melanoma.....	18
2.1.7 Various <i>in-vivo</i> tumor models with special reference to the syngeneic tumor model	20
2.2 Role of plant extracts and phytoconstituents against melanoma	21
2.3 Plant profile of <i>Piper longum</i>	23
2.3.1 Geographical distribution.....	23
2.3.2 Plant description.....	23
2.3.3 Scientific classification	24
2.3.4 Synonyms.....	24
2.3.5 Chemical profile of fruit	25
2.3.6 Pharmacological profile	25
2.3.7 Role of <i>Piper longum</i> fruit extract and contained phytoconstituents against melanoma	26
2.4 Solid dispersion (SD).....	28
2.4.1 Advantages & disadvantages	30
2.4.2 Classification of solid dispersion	31
2.4.3 Excipients used for SD.....	32
2.4.4 The need for SD formulation of herbal extracts, enriched fractions, and isolated bioactive	33
2.4.5 Method of preparation with special reference to solvent method.....	33
2.4.6 Chemistry of CM-phytoconstituents interaction in SD	35
2.4.7 SD of herbal extracts and isolated plant bioactives	35

2.5	Transdermal drug delivery system (TDDS)	36
2.5.1	Novel formulation strategies to avoid the hurdles of transdermal permeation ..	37
2.5.2	Transferosome (TFs).....	38
2.5.3	Methods for formulation of TFs	39
2.5.4	Transgelosome	40
2.5.5	TFG of multiconstituent-based herbal extract and isolated bioactives.....	41
3	CHAPTER 3: RATIONALE AND OBJECTIVES	43
4	CHAPTER 4: MATERIALS, INSTRUMENTS, AND SOFTWARE USED IN THE EXPERIMENTS	45
5	CHAPTER 5: COLLECTION, AUTHENTICATION & EXTRACTION OF <i>PIPER LONGUM</i> FRUITS, AND MARKER-BASED STANDARDIZATION BY VALIDATED HPLC METHOD	51
5.1	Background	51
5.2	Objectives	51
5.3	Methodology	52
5.3.1	Collection and authentication (Taxonomical and Molecular) of <i>Piper longum</i> fruits.....	52
5.3.2	Extraction of <i>Piper longum</i> fruits and residual solvent analysis by Headspace Gas Chromatography (GC-HS) analysis.....	54
5.3.3	Marker-based standardization of PLFEE by validated HPLC as per ICH Topic Q 2 (R1)	56
5.4	Results and Discussion	59
5.4.1	Taxonomical and Molecular authentication of collected <i>Piper longum</i> fruits ..	59
5.4.2	Extraction of <i>Piper longum</i> fruits and residual solvent analysis	63
5.4.3	Marker-based standardization of PLFEE by validated HPLC as per ICH Topic Q 2 (R1)	65
5.5	Conclusions	79
5.6	Summary points:	79
6	CHAPTER 6: DEVELOPMENT, OPTIMIZATION, AND CHARACTERIZATION OF FOURTH-GENERATION TERNARY SOLID DISPERSION OF STANDARDIZED <i>PIPER LONGUM</i> FRUIT EXTRACT FOR MELANOMA THERAPY	81
6.1	Background	81
6.2	Objectives	82

6.3 Methodology	82
6.3.1 Screening of carrier matrix (CM) by phase solubility experiment	82
6.3.2 Formulation of SD	83
6.3.3 Quality by design (QbD) and optimization.....	84
6.3.4 Characterizations of optimized SD	86
6.3.5 <i>In-vitro</i> cytotoxicity assay.....	95
6.3.6 Cell migration assay (<i>in-vitro</i> wound healing assay).....	97
6.3.7 Approved protocol for standard experimental animals' conditions.....	98
6.3.8 <i>In-vivo</i> oral Bioavailability study.....	98
6.3.9 Acute oral toxicity study (LD ₅₀)	105
6.3.10 <i>In-vivo</i> anticancer activity in melanoma (B16F10) bearing C57BL/6 mice	107
6.3.11 Statistical analysis.....	110
6.4 Result and Discussions.....	110
6.4.1 Phase solubility study	110
6.4.2 Formulation of SD	116
6.4.3 Quality by design (QbD) and optimization.....	119
6.4.4 Characterizations of optimized solid dispersion (SD)	134
6.4.5 <i>In-vitro</i> cytotoxicity	159
6.4.6 Cell migration assay (<i>in-vitro</i> wound healing assay).....	163
6.4.7 <i>In-vivo</i> oral bioavailability	165
6.4.8 Acute oral toxicity study.....	177
6.4.9 <i>In-vivo</i> anticancer activity against melanoma.....	181
6.5 Conclusions.....	192
6.6 Summary points	193
7 CHAPTER 7: DEVELOPMENT AND CHARACTERIZATION OF TRANSGELOSOME OF STANDARDIZED <i>PIPER LONGUM</i> FRUIT EXTRACT FOR MELANOMA THERAPY	195
7.1 Background	195
7.2 Objectives.....	196
7.3 Methodology	196
7.3.1 Formulation and Development of transferosome (TFs) of standardized PLFEE 196	
7.3.2 Response surface methodology (RSM) and optimization	197
7.3.3 Characterization of TFs.....	198
7.3.4 Formulation of TFG, placebo TFG, and plain gel	208
7.3.5 Characterization of TFG	208
7.3.6 Approved protocol for standard experimental animals' conditions.....	212
7.3.7 <i>Ex-vivo</i> skin permeation study and permeability kinetics.....	213
7.3.8 Depth of skin penetration via confocal laser scanning microscopy (CLSM) microscopy.....	215

7.3.9	Acute dermal toxicity of standardized PLFEE	216
7.3.10	Skin irritation study.....	217
7.3.11	<i>In-vivo</i> anticancer activity in melanoma (B16F10) bearing C57BL/6 mice	218
7.3.12	Statistical analysis.....	219
7.4	Results and Discussion.....	219
7.4.1	Formulation development of TFs.....	219
7.4.2	Optimization	221
7.4.3	Characterization of TFs.....	247
7.4.4	Characterization of gel.....	271
7.4.5	Ex-vivo skin permeation study and permeability kinetics.....	287
7.4.6	Depth of skin penetration via confocal laser scanning microscopy (CLSM) ..	292
7.4.7	Acute dermal toxicity of standardized PLFEE	295
7.4.8	Skin irritation study.....	301
7.4.9	<i>In-vivo</i> anticancer activity against melanoma.....	305
7.5	Conclusions.....	311
7.6	Summary points	312
8	CHAPTER 8: COMBINED <i>IN-VIVO</i> ANTICANCER ACTIVITY EVALUATION OF OPTIMIZED SD AND TFG AGAINST MELANOMA.....	315
8.1	Background	315
8.2	Objectives.....	315
8.3	Methodology	316
8.3.1	Approval for animal experiments and standard experimental conditions	316
8.3.2	<i>In-vivo</i> anticancer activity of optimized SD and TFG in melanoma-bearing C57BL/6 mice.....	316
8.3.3	Statistical analysis.....	317
8.4	Results and Discussion.....	317
8.4.1	<i>In-vivo</i> anticancer activity of optimized SD and TFG in melanoma-bearing C57BL/6 mice.....	317
8.5	Conclusions.....	322
8.6	Summary points	323
9	CHAPTER 9: SUMMARY AND CONCLUSION.....	325
	REFERENCES.....	329
10	APPENDICES.....	343
10.1	Appendix A: Taxonomical authentication of <i>Piper longum</i> fruits.....	343

10.2	Appendix B: Institutional Animal Ethic Committee (IAEC) Certificates....	344
10.3	Appendix C: Acute oral toxicity report of standardized extract.....	347
10.4	Appendix D: Publications.....	348
10.4.1	List of publications from the Thesis work	348
10.4.2	List of other publications during the research work	348
10.5	Appendix E: Skills learned during Ph.D. tenure	354

List of Figures

Figure 2. 1 Anatomy of the skin, showing the epidermis, dermis, and subcutaneous tissue. Melanocytes are in the layer of basal cells at the deepest part of the epidermis.	9
Figure 2. 2 Estimated No. of new cases of melanoma of skin in 2020 as per Global Cancer Observatory (GCO)-2020 data base (a) overall estimated no of new cases of melanoma of skin in both sexes at all ages and (b) estimated no of new cases of melanoma of skin in male and female at all ages.	11
Figure 2. 3 Estimated No. of death due to melanoma of skin in 2020 in world as per GCO-2020 data base (a) overall estimated no of death due to melanoma of skin in both sexes at all ages and (b) estimated no of death due to melanoma of skin in male and female at all ages.	12
Figure 2. 4 Melanomas with characteristic asymmetry, border irregularity, color variation, and large diameter (ABCD).	14
Figure 2. 5 Mitogen-activated protein kinase (MAPK pathway) and phosphoinositide-3-OH kinase (PI3K/Akt)	17
Figure 2. 6 Mechanism of action of various plant extracts and active phytoconstituents against melanoma.....	22
Figure 2. 7 Photograph of (a) <i>Piper longum</i> plant and (b) fruits	24
Figure 2. 8 Role of <i>Piper longum</i> in melanoma therapy.....	27
Figure 2. 9 The mechanism behind enhanced solubility, dissolution, absorption, bioavailability, and elevated therapeutic activity of solid dispersion	30
Figure 2. 10 Need for SD formulation of herbal extracts, enriched fractions, and isolated bioactives	33
Figure 2. 11 Various methods of preparation of SD.....	34
Figure 2. 12 Structure of skin	37
Figure 2. 13 Composition & structure of transferosome	38
Figure 2. 14 Advantages of TFs.....	39
Figure 2. 15 Formulation methods of TFs	40
Figure 5. 1 Schematic representation of workflow of chapter 5.....	52
Figure 5. 2 Gel electrophoresis and DNA sequencing chromatogram (a) gel electrophoresis results under UV light using a gel documentation system: Left Lane: 2-log DNA ladder and right lane: the PCR amplification fragment of <i>rbcL</i> , (b) DNA sequencing chromatogram of <i>rbcL</i> gene.	62
Figure 5. 3 Schematic representation of extraction of <i>Piper longum</i> fruits.....	64
Figure 5. 4 GC-HS analysis for residual ethanol content (a) GC-HS-chromatogram of absolute ethanol with the retention time of 2.04 min and the inset image showing the calibration plot, (b) chromatogram of ethanol in the dried extract (PLFEE).....	65
Figure 5. 5 HPLC chromatograms and absorption spectra of PIP and PPLGN each of 28 µg/mL in mobile phase methanol and water (80:20 v/v) (a) chromatogram of PIP (Rt = 7.087 ± 0.053 min) at wavelength 342 nm, (b) chromatogram of PLGN (Rt = 6.413 ± 0.014 min) at wavelength 340 nm, (c) spectrum of PIP showing the maximum absorbance at 342 nm, and (d) spectrum of PLGN showing the absorption maxima at 340 nm	66
Figure 5. 6 Two-dimensional (2-D) and three-dimensional (3-D) chromatograms of PIP and PLGN (a) 2-D contour chromatogram of PIP (b) 3-D chromatogram of PIP, (c) 2-D contour chromatogram of PLGN, and (d) 3-D chromatogram of PLGN.....	67

Figure 5. 7 HPLC-based calibration curves (a) calibration curve of PIP measured at wavelength 342 nm and (b) calibration curve of PLGN measured at wavelength 340 nm	68
Figure 5. 8 Purity curve of PIP and PLGN (a) purity curve of PIP and (b) purity curve of PLGN	76
Figure 5. 9 HPLC results of PLFEE 1mg/mL and 50µg/mL in mobile phase methanol and water (80:20 v/v) (a) Chromatograms of PIP (Rt = 7.087 ± 0.023 min) and PPLGN (Rt = 6.340 ± 0.046 min) in 1 mg/mL of PLFEE at wavelength 340 nm (b) Chromatogram of PIP (Rt = 7.087 ± 0.023 min) at wavelength 342 nm and chromatogram of PLGN (Rt = 6.333 ± 0.027 min) at wavelength 342 nm, (c) spectrum of PLGN in 1 mg/mL of PLFEE showing the maximum absorbance at 340 nm, (d) spectrum of PIP in 50 µg/mL of PLFEE showing the absorption maxima at 342 nm, (e) 2-D contour chromatogram of PIP and PLGN in 1 mg/mL of PLFEE (f) 2-D contour chromatogram of PIP and PLGN in 50 µg/mL of PLFEE, (g) 3-D chromatogram of PIP and PLGN in 1 mg/mL of PLFEE, and (h) 3-D chromatogram of PIP and PLGN in 50 µg/mL of PLFEE.....	78
Figure 6. 1 Schematic representation of workflow of chapter 6.....	82
Figure 6. 2 Phase solubility of PIP from <i>Piper longum</i> fruits ethanolic extract (PLFEE) in various carrier matrices (CMs) (a) solubility of PIP in polymers and surfactants (b) solubility in polymers, (c) solubility in surfactants, (d) A _N type phase diagram of Soluplus [®] , and (e) A _L type phase diagram of Tween [®] 80. Each value represents the solubility of PIP in 2, 4, and 8% (w/v) aqueous solution of carriers and is represented as mean ± S.D. (n = 3).	113
Figure 6. 3 Chemical structure and micellar solubilization properties of Soluplus [®] and Tween [®] 80 (a) the chemical structure and schematic illustration of the micellar solubilization of hydrophobic candidates by Soluplus [®] (b) the chemical structure and schematic illustration of the micellar solubilization of hydrophobic candidates by Tween [®] 80.....	115
Figure 6. 4 Formulation development of SDs and formulation consequences (a) various steps involved during the development of PLFEE loaded SDs, (b) sticky product, (c) rubbery film type product, and (d) highly porous dried thin film of formulation.	118
Figure 6. 5 Diagnostic plots and perturbation plot (a) normal plot of residuals and (b) Box-Cox plot.....	126
Figure 6. 6 Diagnostic plots and perturbation plot (a) predicted vs. actual plot and (b) residual vs. predicted plot	127
Figure 6. 7 Diagnostic plots and perturbation plot (a) residual vs. run and (b) residual vs. factor plot.....	128
Figure 6. 8 Perturbation plot for saturation solubility of PIP	129
Figure 6. 9 Three-dimensional response surface plots and corresponding counterplots for saturation solubility (a and b) effect of factor X ₁ and X ₂ , considering factor X ₃ constant (c and d) effect of factor X ₁ and X ₃ , considering factor X ₂ constant, and (e and f) effect of factor X ₃ and X ₂ , considering factor X ₁ constant	131
Figure 6. 10 Constrains and solutions to achieve CQA (a) criteria for achieving maximum saturation solubility and (b) one of the software-generated solutions out of 56 solutions, and (c) overlay plot as a function of change in X ₁ and X ₂ , considering X ₃ constant	133
Figure 6. 11 XRD diffractograms of optimized SD and formulation components (PLFEE, Soluplus [®] , Tween [®] 80, and PM).....	137

Figure 6. 12 DSC thermograms of PLFEE, Soluplus [®] , PM, and optimized SD	139
Figure 6. 13 TGA thermograms of PLFEE, Soluplus [®] , PM, and optimized SD.....	141
Figure 6. 14 ATR-FTIR results of SD, PLFEE, Soluplus [®] , Tween [®] 80, PM, optimized SD, PM of formulation F4, and SD F4	143
Figure 6. 15 HPTLC fingerprints of PIP, PLGN, PLFEE, PM, and SD (a) fingerprint under 254 nm, (b) fingerprint under 366 nm, and (c) fingerprint under visible light.....	147
Figure 6. 16 Contact angle measurements (a) mean contact angle (θ_M) of 10 individual droplets, (b) contact angle of the water droplet on SD film, and (c) contact angle of the water droplet on PLFEE film.....	148
Figure 6. 17 HRSEM results of (a) PLFEE, (b) Soluplus [®] , (c) PM, (d) SD, (e) PLFEE dried on a slide, and (f) SD dried on a slide.....	150
Figure 6. 18 PLM photomicrographs of PLFEE, Soluplus [®] , PM, and SD at 10X magnification	151
Figure 6. 19 <i>In-vitro</i> dissolution study of PLFEE, PM, and optimized SD in pH 1.2. Each analysis was carried out in triplicate, and the results were represented as mean \pm standard deviation.....	153
Figure 6. 20 The hypothesized diagram of the micelles of OSD during dissolution.....	154
Figure 6. 21 Hydrodynamic particle size, polydispersity index, and zeta potential on formed micelles during dissolution (a) Z_{avg} , (b) correlogram, (c) ζ , and (d) phase plot	156
Figure 6. 22 HRTEM and SAED results of produced micelles in pH 1.2 dissolution media (a) HRTEM photomicrograph of micelles at 0.5 μ M scale, (b) size distribution, (c) HRTEM photomicrograph of micelles at 200 nm scale, and (f) SAED pattern	157
Figure 6. 23 Accelerated stability study of optimized SD up to 6 months at an interval of 3 months (a) XRD, (b) DSC, (c) TGA, and (d) ATR-FTIR	159
Figure 6. 24 Cytotoxicity studies (a) cytotoxicity of PLFEE suspension, PLFEE solution, and optimized SD against B16F10 after 24 h, (b) cytotoxicity of DTIC against B16F10 after 24 h, (c) log (concentration) of PLFEE suspension, PLFEE solution, and optimized SD v/s viability (%) of B16F10 after 24 h, (d) log (concentration) of DTIC v/s viability (%) of B16F10 after 24 h, (e) cytotoxicity of PLFEE suspension, PLFEE solution, and optimized SD against HEK 293 cells after 24 h, and (f) cytotoxicity of DTIC against HEK293 after 24 h. Each data point represents the mean \pm SD of three independent experiments.	162
Figure 6. 25 <i>In-vitro</i> cell migration assay (a) inhibitory effect of PLFEE and optimized SD on the motility of B16F10 cells and (b) percentage cell migration in the presence of PLFEE and optimized SD. Each data point represents the mean \pm SD of three independent experiments. The statistical analysis was carried out using one-way ANOVA followed by Tukey's multiple comparison test at $p < 0.05$	164
Figure 6. 26 Chromatograms of PIP (1.6 μ g/mL) and p-DMAB (1 μ g/mL) in mobile phase methanol and water (80:20 v/v) (a) chromatogram of PIP ($R_t = 7.02 \pm 0.062$ min) and p- DMAB ($R_t = 4.113 \pm 0.026$ min) at wavelength 342 nm, (b) DAD absorption spectrum of PIP having $\lambda_{max} = 342$ nm (c) DAD absorption spectrum of p-DMAB having $\lambda_{max} = 346$ nm, (d) 2-D contour chromatogram of PIP and p-DMAB, and (e) 3-D chromatogram of PIP and p-DMAB	166
Figure 6. 27 Calibration curve and selectivity study (a) calibration curve of PIP in plasma at wavelength 342 nm with p-DMAB as IS, (b) HPLC chromatograms of blank rat plasma, (c) plasma spiked with p-DMAB (0.354 μ g/mL), (d) plasma spiked with PIP (25.6 μ g/mL),	

(e) plasma spiked with p-DMAB (1 $\mu\text{g/mL}$) and PIP (25.6 $\mu\text{g/mL}$), and (f) extracted plasma sample after oral administration of optimized solid dispersion (OSD) with the p-DMAB (1 $\mu\text{g/mL}$) as internal standard	167
Figure 6. 28 Plasma drug concentration-time profile after oral administration of PLFEE, PM, and SD each equivalent to 62.83 mg/kg of PIP in female SD rats (n = 5, Mean \pm SD)	175
Figure 6. 29 Histopathology study of heart, kidney, liver, lungs, and spleen of (a) vehicle control C57BL/6 group and (b) PLFEE (550 mg/kg) treated C57BL/6 group at 10X magnification for acute oral toxicity assessment. BM: branching myocytes; G: glomerulus; CV: central vein; B: bronchioles; RP: red pulp; and WP: white pulp. The histopathological observations were obtained from the vital organs of the vehicle control C57BL/6 group and PLFEE (550 mg/kg) treated C57BL/6 group, each comprising 4 animals/group. The histological photomicrographs and descriptions are based on the histology of six replicate organ sections of each organ.....	180
Figure 6. 30 Tumor regression analysis (a) changes in body weight, (b) tumor volume at an interval of two days after developed palpable tumor, (c) tumor volume at the end of dosing (30 th day), (d) tumor volume doubling time (VDT) of various group, (e) tumor weight at 30 th day, (f) percent tumor growth inhibition (% TGI) of various groups at 30 th day. The asterisk marks (*) represent the level of significance at $p < 0.05$ in all cases. The statistical analysis for the oral bioavailability and tumor regression analysis was performed using one-way ANOVA followed by Tukey's multiple comparison test at $p < 0.05$ using GraphPad Prism 5 (GraphPad Software, Inc., San Diego, California).	182
Figure 6. 31 Tumor photograph and survival plot (a) photograph of representative tumors from each group on the 30 th day and (b) Kaplan-Meier survival plot.	186
Figure 6. 32 Histopathology study of skin and melanoma tumor: histology of (a) normal skin, (b) skin over melanoma tumor, (c) tumor control, (d) tumor of DTIC treated, (e) tumor of PLFEE treated, (f) tumor of SD treated, (g) tumor of DTIC + PLFEE treated, and (h) tumor of DTIC + SD treated group. NR: necrotic region; LTC: live tumor cell. The histopathological observations were obtained from the skin and tumors of each animal from seven different groups (5 animals/group). All the histological interpretations are based on the photomicrographs and observations from six replicate sections of each specimen...	188
Figure 7. 1 Schematic representation of workflow of Chapter 7.....	196
Figure 7. 2 In-house fabricated device for the flexibility determination of TFs.....	201
Figure 7. 3 Formulation methodology of standardized PLFEE-loaded TFs by thin film hydration method.	221
Figure 7. 4 Twenty formulations of standardized PLFEE-loaded TFs as per the design of experiment.....	221
Figure 7. 5 Diagnostic plots for response Y ₁ : Vesicle Size (Z_{avg}) (a) normal plot of residuals and (b) Box-Cox plot.....	230
Figure 7. 6 Diagnostic plots for response Y ₁ : Vesicle Size (Z_{avg}) (a) predicted vs. actual plot and (b) residual vs. predicted plot.....	231
Figure 7. 7 Diagnostic plots for response Y ₁ : Vesicle Size (Z_{avg}) (a) residual vs. run and (b) residual vs. factor plot	232
Figure 7. 8 Diagnostic plots for response Y ₂ : % Entrapment Efficiency (% EE) (a) normal plot of residuals, and (b) Box-Cox plot	233
Figure 7. 9 Diagnostic plots for response Y ₂ : % Entrapment Efficiency (% EE) (a) predicted vs. actual plot and (b) residual vs. predicted plot.....	234

Figure 7. 10 Diagnostic plots for response Y ₂ : % Entrapment Efficiency (% EE) (a) residual vs. run and (b) residual vs. factor plot.....	235
Figure 7. 11 Diagnostic plots for response Y ₃ : Flexibility (a) normal plot of residuals, and (b) Box-Cox plot.....	236
Figure 7. 12 Diagnostic plots for response Y ₃ : Flexibility (a) predicted vs. actual plot and (b) residual vs. predicted plot.....	237
Figure 7. 13 Diagnostic plots for response Y ₃ : Flexibility (a) residual vs. run and (b) residual vs. factor plot.....	238
Figure 7. 14 Perturbation plots (a) perturbation plot for Y ₁ , (b) perturbation plot for Y ₂ , and (c) perturbation plot for Y ₃	240
Figure 7. 15 3D response surface plots for vesicle size (a) effect of Tween [®] 80 and PL-90H on vesicle size, (b) effect of PL-90H and probe sonication time on vesicle size, and (c) effect of Tween [®] 80 and probe sonication time on vesicle size	242
Figure 7. 16 3D response surface plots for entrapment efficiency (a) effect of Tween [®] 80 and PL-90H on entrapment efficiency, (b) effect probe sonication time and PL-90H on entrapment efficiency, and (c) effect of probe sonication time and Tween [®] 80 on entrapment efficiency.....	244
Figure 7. 17 3D response surface plots for flexibility (a) effect of Tween [®] 80 and PL-90H on flexibility, (b) effect probe sonication time and PL-90H on flexibility, and (c) effect of probe sonication time and Tween [®] 80 on flexibility	246
Figure 7. 18 Overlay plot indicating the optimized formula	247
Figure 7. 19 Vesicle size (Z _{avg}), polydispersity index (PDI), and zeta potential (ζ) of optimized TFs (a) Z _{avg} , PDI, (b) correlogram, (c) ζ, and (d) phase plot.....	248
Figure 7. 20 Morphology analysis through optical microscopy and HRSEM (a) optical photomicrograph of TFs before probe sonication at 10X magnification, (b) optical photomicrograph of optimized TFs at 10X magnification, (c) optical photomicrograph of optimized TFs at 4X magnification, and (d) HRSEM photomicrograph of optimized TFs	250
Figure 7. 21 Morphology analysis through SPM and HRTEM (a) 2D SPM photomicrograph of optimized TFs, (b) 3D SPM photomicrograph of optimized TFs, (c) HRTEM photomicrograph of TFs before probe sonication at 2 μm scale, (d) HRTEM photomicrograph of optimized TFs at 100 nm scale, (e) HRTEM photomicrograph of optimized TFs at 2 μm scale, and (f) SAED pattern of optimized TFs	251
Figure 7. 22 Drug-excipient compatibility analysis in optimized TFs by ATR-FTIR (a) fingerprint under 254 nm, (b) fingerprint under 366 nm, and (c) fingerprint under visible light.....	254
Figure 7. 23 Drug-excipient compatibility analysis in optimized TFs by HPTLC (a) fingerprint under 254 nm, (b) fingerprint under 366 nm, and (c) fingerprint under visible light.....	255
Figure 7. 24 PLM photomicrographs of PLFEE, PL-90H, physical mixture, and TFs FD at 10X magnification	257
Figure 7. 25 XRD diffractograms of optimized freeze-dried TFs (TFs FD), formulation components (PLFEE, PL-90H, Tween [®] 80), and physical mixture	258
Figure 7. 26 DSC thermogram of optimized freeze-dried TFs (TFs FD), formulation components (PLFEE, PL-90H), and physical mixture	260

Figure 7. 27 TGA thermogram of optimized freeze-dried TFs (TFs FD), formulation components (PLFEE, PL-90H), and physical mixture	261
Figure 7. 28 Cytotoxicity studies (a) cytotoxicity of PLFEE and optimized TFs against B16F10 after 24 h with the inset figure showing the log of concentrations v/s % cell viability, (b) cytotoxicity of PLFEE and optimized TFs against HEK293 after 24 h	267
Figure 7. 29 Cellular uptake studies (a) cellular uptake of CU-6 and CU-6-TFs in B16F10 cells after 1 h and (b) quantitative graph of fluorescence intensity of CU-6 and CU-6-TFs in B16F10 cell line in terms of total area and mean gray value statistically analyzed by unpaired t-test at 95% significance level	268
Figure 7. 30 <i>In-vitro</i> cell migration assay (a) inhibitory effect of PLFEE and optimized TFs on the motility of B16F10 cells and (b) percentage cell migration in the presence of PLFEE and optimized TFs. Each data point represents the mean \pm SD of three independent experiments. The statistical analysis was carried out using one-way ANOVA followed by Tukey's multiple comparison test at $p < 0.05$	270
Figure 7. 31 Photographs of prepared gels (placebo TFG F2, plain gel, TFG F1, TFG F2, and TFG F3).....	273
Figure 7. 32 Spreadability study of gels (a) spreadability of TFG F2 and (b) spreadability of marketed gel (Omnigel, Cipla Ltd.).....	274
Figure 7. 33 Rheogram of various gel	276
Figure 7. 34 Amplitude sweep curve of (a) TFG F1, (b) TFG F2, (c) TFG F3, (d) marketed Omnigel, (e) plain gel, and (f) placebo TFG F2 gel	277
Figure 7. 35 Drug excipient compatibility via ATR-FTIR: FTIR spectra of gel formulation components (PLFEE, xanthan gum, water, propylene glycol, methyl paraben, and propyl paraben).....	279
Figure 7. 36 Drug excipient compatibility via ATR-FTIR: FTIR spectra of physical mixture of gel formulations (physical mixture of plain gel and physical mixture of TFG) and gel formulations (freeze dried TFG F1-F3, plain gel, and placebo gel TFG F2)	280
Figure 7. 37 <i>In-vitro</i> release study of optimized TFs, PLFEE solution, plain gel and TFG F2 through dialysis bag.....	282
Figure 7. 38 <i>Ex-vivo</i> skin permeability of plain gel and TFG F2 through C57BL/6 female mice.....	289
Figure 7. 39 Structure of skin and the penetration mechanism of transferosome across the skin (a) anatomy of the skin and (b) mechanism of skin penetration of ultradeformable transferosome	291
Figure 7. 40 CLSM study for the depth of CU-6 penetration into C57BL/6 skin from plain gel loaded CU-6. Each photomicrograph was captured by optical slicing of the skin from the epidermis to subcutaneous tissue by the Z-stacking feature of CLSM and the depth of each layer is marked in the figure.	293
Figure 7. 41 CLSM study for the depth of CU-6 penetration into C57BL/6 skin from TFG F2 loaded CU-6. Each photomicrograph was captured by optical slicing of the skin from the epidermis to subcutaneous tissue by the Z-stacking feature of CLSM and the depth of each layer is marked in the figure.	294
Figure 7. 42 Acute dermal toxicity study for estimation of skin irritancy (a) photograph of vehicle applied control C57BL/6 female mouse, (b) photograph of standardized PLFEE (2000 mg/kg) applied C57BL/6 mouse, (c) histopathology of vehicle applied control	

C57BL/6 female mouse, and (d) histopathology of standardized PLFEE (2000 mg/kg) applied C57BL/6 mouse observed at 10X magnification	296
Figure 7. 43 Histopathology of heart, kidney, liver, lungs, and spleen of (a) vehicle control C57BL/6 group and (b) PLFEE (2000 mg/kg) topically treated C57BL/6 group at 10X magnification for acute dermal toxicity assessment. PLFEE: <i>Piper longum</i> fruits ethanolic extract; BM: branching myocytes; G: glomerulus; CV: central vein; HPV: hepatic portal vein; B: bronchioles; RP: and red pulp; and WP: white pulp	300
Figure 7. 44 Skin irritation study of (a) standard irritant (0.8% w/v aqueous formalin solution), (b) placebo TFG F2, (c) TFG F2, and (d) plain gel. Placebo TFG F2: Placebo transgelosome formulation TFG F2; TFG F2: Transgelosome containing optimized transferosome	302
Figure 7. 45 Histopathological photomicrographs of C57BL/6 mice skin after skin irritation studies of (a) standard irritant (0.8% w/v aqueous formalin solution), (b) placebo TFG F2, (c) TFG F2, and (d) plain gel	304
Figure 7. 46 Tumor regression analysis (a) changes in body weight, (b) tumor volume at an interval of two days after developed palpable tumor, (c) tumor volume on 30 th day, (d) tumor volume doubling time (VDT) of various group, (e) tumor weight at 30 th day, and (f) percent tumor growth inhibition (% TGI) of various groups at 30 th day. The asterisks marks (*) represent the level of significance at p<0.05 in all cases. The statistical analysis was performed using one way ANOVA at followed by Tukey's test p<0.05 using GraphPad Prism 5 (GraphPad Software, Inc., San Diego, California)	307
Figure 7. 47 Photographs of isolated tumor and life expectancy study (a) photograph of representative tumors from each group on 30 th day, (b) life expectancy study	308
Figure 7. 48 Histopathology study of skin and melanoma tumor: histology of (A) normal skin, (B) skin over melanoma tumor, (C) tumor of tumor control, (D) tumor of DTIC treated, (E) tumor of plain gel, (F) tumor of TFG F2 treated, (G) tumor of DTIC + Plain gel treated, and (H) tumor of DTIC + TFG F2 treated group. NR: necrotic region; LTC: live tumor cell	310
Figure 8. 1 Schematic representation of workflow of Chapter 8	315
Figure 8. 2 Tumor regression analysis (a) changes in body weight, (b) tumor volume at an interval of two days after developed palpable tumor, (c) tumor volume on 30 th day, (d) tumor volume doubling time (VDT) of various group, (e) tumor weight at 30 th day, and (f) percent tumor growth inhibition (% TGI) of various groups at 30 th day. The asterisks marks (*) represent the level of significance at p<0.05 in all cases. The statistical analysis was performed using one way ANOVA at followed by Tukey's test p<0.05 using GraphPad Prism 5 (GraphPad Software, Inc., San Diego, California)	321
Figure 8. 3 Photograph of representative tumors from each group on 30 th day	322

List of Tables

Table 2. 1 Chemical profile of <i>P. longum</i> fruit.....	25
Table 2. 2 Studies on <i>Piper longum</i> and their constituents for melanoma therapy.	27
Table 2. 3 Commonly employed excipients/carrier matrix in solid dispersion	32
Table 4. 1 List of materials used and their sources.....	45
Table 4. 2 List of Instruments used.....	48
Table 4. 3 List of software used.....	50
Table 5. 1 Sequence matches the result of the sample sequence with the reported sequence (ID: ON720789.1).....	61
Table 5. 2 Outcomes of BLAST analysis	63
Table 5. 3 Accuracy studies of the developed HPLC method (n = 3)	69
Table 5. 4 Repeatability study of developed HPLC method (n = 6).....	70
Table 5. 5 Intermediate precision (Intra-day and inter-day precision) studies of the developed HPLC method.....	71
Table 5. 6 Robustness and ruggedness study of developed HPLC method for PIP (12 µg/mL)	73
Table 5. 7 Robustness and ruggedness study of developed HPLC method for PLGN (12 µg/mL)	74
Table 5. 8 System suitability study of developed HPLC method for analysis of PIP (12 µg/mL), n = 6	76
Table 5. 9 System suitability study of developed HPLC method for analysis of PLGN (12 µg/mL), n = 6	76
Table 6. 1 Gibbs free energy (ΔG_t°) transfer of PIP from pure water to an aqueous polymeric or surfactant solution.....	116
Table 6. 2 Coded levels, real values for each factor under experiment, and CQA.....	120
Table 6. 3 Central composite design (CCD)-based trial formulation batches with respective CQA.....	121
Table 6. 4 Results of model fit summary and model summary statistics	123
Table 6. 5 ANOVA for quadratic model and fit statistics	124
Table 6. 6 Kinetics of drug release in pH 1.2 up to 24 h	155
Table 6. 7 Accuracy studies of the developed HPLC method for estimation of PIP in plasma (n = 3)	168
Table 6. 8 Precision results of the developed HPLC method for quantification of PIP in plasma	169
Table 6. 9 Percent extraction recovery (PER) of PIP and p-DMAB through the developed HPLC method (n = 3)	170
Table 6. 10 Robustness and ruggedness study of developed HPLC method for estimation of PIP (1.6 µg/mL) in rat plasma	171
Table 6. 11 System suitability study of developed HPLC method for analysis of PIP (12 µg/mL) in rat plasma (n = 6).....	172
Table 6. 12 Stability study reports of analyzed QC samples (n = 3)	173
Table 6. 13 Pharmacokinetic (PK) parameters of PIP following single oral administration of PLFEE, PM, and optimized SD (n = 5, Mean \pm SD)	176
Table 6. 14 Biochemical parameters of vehicle control C57BL/6 group and PLFEE (550 mg/kg) treated C57BL/6 group.....	178

Table 6. 15 Hematological parameters of vehicle control C57BL/6 group and PLFEE (550 mg/kg) treated C57BL/6 group.....	179
Table 7. 1 Coded levels, real values of each factor, and Critical Quality Attributes (CQA).....	222
Table 7. 2 CCD-based TFs formulations with respective responses	223
Table 7. 3 Polydispersity index (PDI), Zeta potential (ζ), loading capacity (LC), pH, and refractive index (RI) of TFs	224
Table 7. 4 Statistical model fit summary	226
Table 7. 5 ANOVA for quadratic model and fit statistics for vesicle size	227
Table 7. 6 ANOVA for quadratic model and fit statistics for entrapment efficiency.....	228
Table 7. 7 ANOVA for quadratic model and fit statistics for flexibility.....	229
Table 7. 8 Validations results of checkpoint batch (n = 5).....	247
Table 7. 9 Long-term stability study of optimized TFs	264
Table 7. 10 Accelerated stability study, freeze-thaw, and heating-cooling stability study of optimized TFs	265
Table 7. 11 Lyophilization stability of optimized TFs	266
Table 7. 12 Composition of transgelosomes, placebo transgelosome, and plain gel.....	271
Table 7. 13 Characterization of transgelosome, plain gel, and placebo transgelosome ..	272
Table 7. 14 Kinetics of drug release from optimized TFs and TFG F2.....	283
Table 7. 15 Long-term stability study of TFG F2 under refrigerated conditions ($5 \pm 3^\circ\text{C}$)	284
Table 7. 16 Long-term stability study of plain gel under refrigerated conditions ($5 \pm 3^\circ\text{C}$)	285
Table 7. 17 Accelerated stability study of TFG F2 at $25 \pm 2^\circ\text{C}/60 \pm 5\% \text{RH}$	286
Table 7. 18 Accelerated stability study of plain gel at $25 \pm 2^\circ\text{C}/60 \pm 5\% \text{RH}$	287
Table 7. 19 <i>Ex-vivo</i> skin permeability of plain gel and TFG F2.....	289
Table 7. 20 Kinetics of drug permeated from TFG F2 through C57BL/6 mice skin	292
Table 7. 21 Grading values for the primary skin irritation test and response categories.	296
Table 7. 22 Reaction on skin and score of vehicle-applied control C57BL/6 female mice, and standardized PLFEE (2000 mg/kg) applied C57BL/6 mice	297
Table 7. 23 Biochemical parameters of topically applied vehicle control C57BL/6 group and standardized PLFEE (2000 mg/kg) treated C57BL/6 group.....	298
Table 7. 24 Hematological parameters of topically applied vehicle control C57BL/6 group and standardized PLFEE (2000 mg/kg) treated C57BL/6 group.....	298
Table 7. 25 Reaction on skin and score of standard irritant (0.8% v/v aqueous formalin solutions), placebo TFG-F2 (vehicle control), TFG-F2, and plain gel on female C57BL/6 mice.....	303

List of Abbreviations

Abbreviations	Description
2FI	Two-factor interaction model
ABC	ATP-binding cassette
ABCD	Asymmetry, border irregularity, color variation, and large diameter
Akt	Ak strain transforming kinase
ALM	Acral lentiginous melanoma
ALP	Alkaline phosphatase
ANOVA	Analysis of variance
AP-1	Activated protein-1
ATR-FTIR	Attenuated total reflectance-Fourier transform infrared spectroscopy
AUC	Area under the curve
b.wt	Body weight
BCC	Basal-cell carcinoma
BLAST	Basic Local Alignment Search Tool
BM	Branching myocytes
BRAF	Serine/threonine-protein kinase B-Rapidly Accelerated Fibrosarcoma
C.V.	Co-efficient of variation
CAP	Cellulose acetate phthalate
CCD	Central composite design
CDER	Center for Drug Evaluation and Research
CDK4	Cyclin-dependent kinase 4
CDKN1A	Cyclin-dependent kinase inhibitor 1A
CDKN2A	Cyclin-dependent kinase inhibitor 2A
CFT	Capillary flow technology

CI	Carr's compressibility index
CLSM	Confocal laser scanning microscopy
CM	Cutaneous melanoma
CM	Carrier Matrices
CMA	Critical material attributes
C_{max}	Maximum plasma concentration
CMC	Carboxy methylcellulose
CMC	Critical micelle concentration
CMEC	Carboxymethylethylcellulose
CMs	Carrier matrices
CMT	Critical micelle temperature
COX-2	Cyclooxygenase 2
CPCSEA	Committee for the Purpose of Control and Supervision of Experiments on Animals
CPP	Critical process parameters
CQA	Critical quality attributes
CREB	Cyclic AMP response element-binding protein
CTLA-4	Cytotoxic T-lymphocyte-associated antigen 4
CU-6-TFs	CU-6 loaded optimized TFs
CV	Central vein
CVM	Center for Veterinary Medicine
DAD	Diode array detector
DM	Desmoplastic melanoma
DMBA	Dimethylbenz[a]anthracene
DMEM/F-12	Dulbecco's Modified Eagle's Medium
dNTPs	Deoxynucleoside triphosphate
DSC	Differential scanning calorimetry

DTIC	Dacarbazine
EA	Edge activators
EE	Entrapment efficiency
EGF	Epidermal growth factor
EGFR	Epidermal growth factor receptor
Er	Enhancement ratio
ERK1/2	Extracellular signal-regulated kinases 1 and 2
ETD	Everhart–Thornley detector
FbD	Formulation by design
FBS	Fetal bovine serum
FDA	Food and Drug Administration
FGF	Fibroblast growth factor
FGFR	Fibroblast growth factor receptor
F _{rel}	Relative bioavailability
GC-HS	Headspace gas chromatography
GCO	Global Cancer Observatory
GDP	Guanosine diphosphate
GEM	Genetically engineered models
GGT	γ -glutamyl transpeptidase
GHS	Globally Harmonised System
GM-CSF	Granulocyte-macrophage colony-stimulating factor
GRAS	Generally Recognized as Safe
GSH	Glutathione
GTP	Guanosine triphosphate
HAADF	High angle annular dark field
HCT	Hematocrit test

HEK 293	Human embryonic kidney 293 cells
HIF-1 α	Hypoxia-inducible factor-1 α
HLB	Hydrophilic–lipophilic balance
HME	Hot-melt extrusion
HPC	Hydroxypropyl cellulose
HPLC	High-performance liquid chromatography
HPMC	Hydroxy propyl methylcellulose
HPMCP	Hydroxypropylmethylcellulose phthalate
HPTLC	High-performance thin layer chromatography
HR	Hausner ratio
HRAS	Harvey rat sarcoma viral oncogene homolog
HRSEM	High-resolution scanning electron microscopy
HRTEM	High-resolution transmission electron microscopy
i.p.	Intra peritoneal
IAEC	Institutional Animal Ethics Committee
ICH	International Conference on Harmonization
IFN	Interferon
IL	Interleukin
ILS	Increase in life span
iNOS	Inducible nitric oxide synthase
IS	Internal standard
J_{\max}	Maximum flux
J_{ss}	Steady-state Flux
K_0	Zero order rate constant
K_1	1 st order rate constant
KDR/Flk-1	Kinase insert domain receptor/fetal liver kinase 1

K_{el}	Elimination rate constant
K_H	Higuchi dissolution constant
K_{HC}	Hixson-Crowell rate constant
K_{kp}	Korsmeyer-Peppas release rate constant
K_p	Permeability coefficient
K_p	Permeation coefficient
LC	Loading Capacity
LD ₅₀	Lethal Dose 50
LLOD	Lower limit of detection
LLOQ	Lower limit of quantification
LMM	Lentigo maligna melanoma
LOD	Limit of detection
LOQ	Limit of quantification
LTC	Live tumor cells
MAPK	Mitogen-activated protein kinase
MC	Methyl cellulose
MCH	Mean corpuscular haemoglobin
MCHC	Mean corpuscular haemoglobin concentration
MCV	Mean corpuscular volume
MEK	Mitogen-activated protein kinase kinase
MEK1/2	MAP kinase extracellular signal regulated kinases 1 and 2
MHC	Major histocompatibility complex
MMP	Matrix metalloproteinases
MRT	Mean residence time
n	Number of repetitions
NCCS	National Centre for Cell Science
NCI	National Cancer Institute

NDDS	Novel drug delivery systems
NF- κ β	Nuclear factor kappa β
NK	Natural killers
NO	Nitric oxide
NR	Necrotic regions
NRAS	Neuroblastoma RAS viral oncogene homolog
OECD	Organization for Economic Co-operation and Development
OFAT	One-factor-at-a-time
OPM	Optimized physical mixture
OSD	Optimized solid dispersion
p.o.	Per oral
PAMAM	Polyamidoamine
PBS	Phosphate-buffered saline
PCNA	Proliferating cell nuclear antigen
PCV	Packed cell volume
PD-1	Programmed cell death protein 1
PDGFR	Platelet-derived growth factor receptor
PD-L1	Programmed cell death ligand 1
p-DMAB	p-dimethylaminobenzaldehyde
PDXs	Patient-derived tumor xenografts
PEG	Polyethylene glycol
PER	Percent extraction recovery
P-gp	P-glycoprotein
PI3K	Phosphatidylinositol-3-kinase
PII	Primary irritation index
PIP	Piperine

PIP2	Phosphatidylinositol- 4, 5-biphosphate
PIP3	Phosphatidylinositol-3, 4, 5-triphosphate
PK	Pharmacokinetic
PKC α	Protein kinase C alpha
PL-90 H	Phospholipon [®] 90 H
PLFEE	<i>Piper longum</i> fruits ethanolic extract
PLGN	Piperlonguminine
PLM	Polarization microscopy
PM	Physical mixture
PPI	Pea protein isolate
PRESS	Predicted Residual Sum of Squares
PTEN	Phosphatase and tensin homolog deleted on chromosome 10
PVA	Polyvinylalcohol
PVDF	Polyvinylidene fluoride
PVP	Polyvinylpyrrolidone
PVP/VA	Poly (vinylpyrrolidone-co-vinyl acetate)
PVP-CL	Crospovidone
PVPPVA	Polyvinylpyrrolidone-polyvinylacetate copolymer
QbD	Quality by design
QC	Quality control
QTPP	Quality target product profile
Raf	Rapidly accelerated fibrosarcoma
Ras	Rat sarcoma virus
RDW	Red cell distribution width
RET	Receptor tyrosine kinase
RP	Red pulp

RSD	Relative standard deviation
RSM	Response surface methodology
Rt	Retention time
RTK	Receptor tyrosine kinase
SAED	Selected area electron diffraction
SC	Stratum corneum
SCC	Squamous-cell carcinoma
SCID	Severe combined immune-deficient
SD	Solid dispersion
SD	Standard deviation
SDC	Sodium deoxycholate
SGOT	Serum glutamic-oxaloacetic transaminase
SGPT	Serum glutamic pyruvic transaminase
SLS	Sodium lauryl sulfate
SPM	Scanning probe microscopy
$t_{1/2}$	Elimination half-life
T-80	Tween [®] 80
TBE	Tris-borate-Ethylenediaminetetraacetic acid
TCR	T-cell receptor
TDDS	Transdermal drug delivery system
TFG	Transgelosome
TFs	Transferosomes
TFs FD	Freeze-dried optimized TFs
TGA	Thermogravimetric analysis
TGF	Transforming growth factor
TGI	Tumor growth inhibition
TILs	Tumor infiltrating T lymphocytes

TIMP	Tissue Inhibitor of Metalloprotease
TLC	Total leucocyte count
T_{max}	Time to reach maximum concentration
TMF	5,7,4'trimethoxyflavone
TNF	Tumor necrosis factor
TO	Turmeric Oleoresin
TPA	12-O-Tetradecanoylphorbol-13-acetate
TRBCs	Total red blood cell counts
TV	Tumor volume
UDP	Up-and-down-procedure
US-FDA	United States Food Drug Administration
UV	Ultraviolet
VDT	Volume doubling time
VEGF	Vascular endothelial growth factor
WBC	White blood cells
WP	White pulp
XRD	X-ray diffraction
Z_{avg}	Vesicular size
ΔG_t	Gibbs free energy transfer

List of symbols

Symbols	Description
%	Percentage
°	Degree
α	Alpha
μ	Micro
β	Beta
γ	Gamma
μg	Microgram
mm	Milli meter
cm	Centi meter
>	Greater than
<	Less than
↑	Increase
↓	Decrease
°C	Degree Celsius
T_g	Glass transition temperature
MW	Molecular weight
®	Registered trademark
TM	Trademark
μL	Micro liter
mAU	Milli-absorbance unit
ppm	Parts per million
v	Volume
nm	Nano meter
λ_{max}	Absorption maxima

bp	Base pair
kH	Kilohertz
W	Watt
min	Minute
#	Mesh size
rpm	Rotation per minute
θ	Theta
g	Gram
mg	Milli gram
cm	Centi meter
w	Weight
s	Second
h	Hour
ζ	Zeta potential
mV	Milli volt
mg/dL	Milligram/deciliter
U/L	Unit/liter
g/dL	Gram/deciliter
fL	Femtoliters
pg	Picogram

Preface

The extract of the *Piper longum* fruit (Long pepper, Family- Piperaceae) and its phytoconstituents have been well investigated to possess anticancer activity against melanoma through *in-vitro* and *in-vivo* tumor models. Irrespective of reported anticancer activity, the poor aqueous solubility of the majority of contained phytoconstituents and the obstruction by major skin barrier, i.e., stratum corneum (SC) of skin restrict their therapeutic use through oral and transdermal routes, respectively. To improve its therapeutic properties against melanoma, two formulations, solid dispersion (SD) and transgelosome (TFG) of standardized *Piper longum* fruits ethanolic extract (PLFEE) were developed and optimized using Quality-by-Design (QbD). To maintain batch-to-batch consistency and provide dose uniformity, the PLFEE was standardized with respect to piperine (PIP) and piperlonguminine (PLGN) by high-performance liquid chromatography (HPLC). Acute oral toxicity and acute dermal toxicity of standardized PLFEE were carried out using healthy nulliparous and non-pregnant female C57BL/6 mice as per Organization for Economic Co-operation and Development (OECD) 425 and OECD 402 guidelines, respectively. The influence of various independent formulation factors on responses were statistically analyzed by response surface methodology (RSM) using 3-factor, 5 levels rotatable central composite design (CCD). The optimized SD and TFG was investigated for pharmaceutical and therapeutic activity against melanoma (B16F10) bearing C57BL/6 female mice. The anticancer activities of novel phytoformulations were also investigated with the standard anticancer drug dacarbazine (DTIC) as an adjuvant therapy. Further, the simultaneous administration of per oral SD and topical TFG formulations was carried out to investigate the *in-vivo* anticancer activity.

The thesis is divided into **nine chapters**, which are as follows:

Chapter 1: Introduction

Chapter 2: Literature review

Chapter 3: Rationale and objectives

Chapter 4: Materials, instruments, and software used in the experiments

Chapter 5 Collection, authentication, extraction of *Piper longum* fruits, and marker-based standardization by validated HPLC method

Chapter 6: Development, optimization, and characterization of fourth-generation ternary solid dispersion of standardized *Piper longum* fruit extract for melanoma therapy

Chapter 7: Development, and characterization of transgelosome of standardized *Piper longum* fruit extract for melanoma therapy

Chapter 8: Combined *in-vivo* anticancer activity evaluation of optimized SD and TFG against melanoma

Chapter 9: Summary and conclusion

Chapter 5, 6, 7 and 8 have “Summary points”, that summarize the key outcomes of the respective chapters.